NorCal Open Access Publications
Journal of Dermatologic Surgery, Research and Therapy
Volume 2, Issue 2
Silver FH, et al.

Research Article

Biomechanical Relationship Between Cells and Collagen in Skin and Skin Lesions

Frederick H Silver[1,2*], Nikita Kelkar[2], Tanmay Deshmukh[2] and Ruchit Shah[2]

[1]Department of Pathology and Laboratory Medicine, Robert Wood Johnson Medical School, Rutgers, The State University of New Jersey, Piscataway, New Jersey, USA

[2]OptoVibronex, LLC., Allentown, Pennsylvania, USA

[*]**Corresponding author:** Frederick H Silver, Department of Pathology and Laboratory Medicine, Robert Wood Johnson Medical School, Rutgers, the State University of New Jersey, Piscataway, New Jersey, USA, E-mail: silverfr@rutgers.edu

Received Date: 19 October, 2019; **Accepted Date:** 15 November, 2019; **Published Date:** 20 November, 2019

Abstract

We have used vibrational optical coherence tomography to study the relationship between cellular and collagen mechanical behavior in skin *in-vivo*. Quantitative measurements of the cellular and collagen resonant frequencies and peak heights were used to calculate the moduli and relative contribution of cells and collagen to the mechanical behavior of skin. Our results suggest that the resonant frequencies measured in vascularized skin are increased by arterial blood flow and is hypothesized to be a result of upregulation of mechanotransduction. The increased cell contribution to the pixel intensity and an increased resonant frequency peak height, suggests that arterial flow influences the mechanical behavior of skin. In comparison, areas of skin not in close proximity to an artery show a reduced cellular resonant frequency peak height. When the ratio of the cellular to collagen resonant frequency peak heights is examined, the results suggest that the cellular peak height increases both in vascularized areas of skin as well as in cancerous lesions. In cancerous lesions the collagen peak is also widened reflecting changes in the amount of collagen and its organization.

It is known that collagen fiber fragmentation and genetic mutations associated with exposure to UV light precede skin lesion formation. It is proposed that these changes alter the cell-cell and cell-collagen biomechanical balance. This alteration upregulates collagen catabolism and cellular division *via* changes in mechanotransduction at the cell-ECM interface. These changes lead to increased cell division and remodeling of the collagen in the extracellular matrix and changes in the mechanical balance between forces transmitted *via* integrin-collagen and cadherin-cadherin interactions. It is proposed that changes in the force balance between cell-extracellular matrix and cell-cell interactions activate phosphokinase pathways that alter skin extracellular matrix metabolism and lead to skin lesion formation.

Keywords: Epidermis; Skin; Collagen; Resonant frequency; Modulus; Stiffness; Mechanical properties; Virtual biopsy; Pixel intensity; Integrins; Cadherins; Mechanotransduction.

Abbreviations:

ECM: Extracellular Matrix

OCT: Optical Coherence Tomography

VOCT: Vibrational Optical Coherence Tomography

Introduction

Gravity plays a central role in vertebrate development and evolution, tissue repair, and regeneration responses. In the presence of a gravitational field, muscular forces required for locomotion or for daily activities are increased [1]. External loading in a gravitational field leads to induction of pathways that modify cell division and protein synthesis [1]. The results of several studies suggest that tissue regeneration and repair may in part be stimulated by external mechanical loading [2-7]. This has led to the observation that the cellular control mechanisms by which environmental influences, such as exposure to UV light, affect cell behavior operate *via* the phosphokinase pathways that are also influenced by external mechanical loading [1].

Many studies have evaluated the effects of mechanical loading at the cellular and tissue levels *in vitro*; however, few studies have been effective in understanding the state of mechanical loading *in vivo.* Changes in the extracellular matrix (ECM) affect the cell and collagen contents and biomechanics of skin [8]. While finite element modeling provides some assistance in interpreting clinical data, many of these studies do not offer information that can be used during a clinical exam to evaluate skin lesions. Therefore, it is important to develop methods that will aid in understanding the biomechanical changes that occur in skin during aging and in disease.

Recently, we have developed a technique to combine optical coherence tomography (OCT) with vibrational analysis (VOCT) to image and analyze the biomechanical properties of tissues non-invasively and non-destructively [9-15]. The result of this analysis is a "virtual biopsy" of skin along with a physical analysis of the major components of the epidermis and dermis [9-17]. These measurements combined with *in vitro* calibration data can be used to interpret mechanical measurements made *in vivo* [9-18]. VOCT has been used to image and measure the mechanical properties of skin and skin cancers, benign skin lesions, bovine cartilage and bone, decellularized human dermis, human cornea and sclera and synthetic polymers as recently reported [9-18]. One interesting observation is that the height of the cellular resonant frequency peak is difficult to measure in normal skin and scar tissue; while the height of the cellular resonant frequency peak increases in size in both benign and cancerous lesions [16, 18]. It has been proposed that the ratio of the heights of the cellular and collagen resonant frequency peaks can be used to differentiate between benign, pre-and cancerous lesions [16, 18].

In this paper we report data on the use of VOCT to determine the heights of the cellular and collagen resonant frequency peaks found in different anatomical locations in human skin. This data is used to explain changes in the cellular peak and the spreading of the collagen peak that is observed in skin lesions [16, 18].

Methods

VOCT Measurements

Image Collection

OCT cross-sectional images were obtained using an OQ Labscope (Lumedica Inc., Durham, NC) modified to do VOCT [9-18].

OCT and Vibrational Analysis *In Vivo*: Transverse sample displacement was generated by placing a speaker near the skin as discussed previously [9-18]. The spectral-domain optical coherence tomography (SD-OCT) system uses a fiber-coupled superluminescent diode light source with an 810 nm center wavelength and 100 nm bandwidth (full-width at half maximum) [9-18].

In vivo studies on the mechanical properties of skin were conducted by placing a blue tooth activated speaker next to the area of tissue to be studied. All studies were conducted at 75 °F and 40% to 50% relative humidity. A frequency generating app was downloaded onto the computer. This app was capable of driving the speaker between 30 and 20,000 Hz. The speaker was placed in several locations near skin on the face and wrist. During *in vivo* measurements, no sensation of the light or sound impinging on the skin was felt. The speaker was placed near the face and over the radial artery of the hand to collect data on different areas of skin in the presence and absence of an artery.

The resonant frequency of each sample was determined by measuring the transverse displacement resulting from sinusoidal driving frequencies ranging from 30 Hz to 300 Hz, in steps of 10 Hz. The peak frequency (the resonant frequency), f_n, was defined as the frequency at which the displacement was maximized. The moduli of skin and radial artery were calculated from measurements of the resonant frequency and tissue thickness made using VOCT and images of the tissues. Moduli were then obtained from a calibration curve that relates resonant frequency and thickness to modulus values (Figure 1). The moduli of each sample were obtained by determination of the resonant frequency from

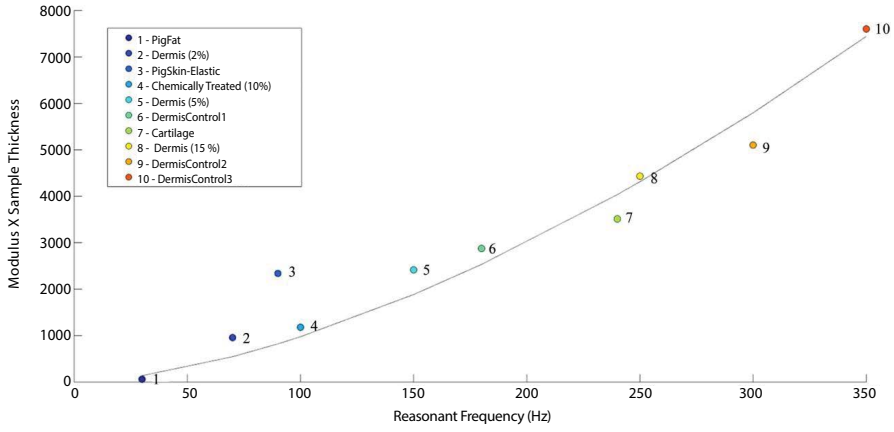

Figure 1: Calibration curve showing the relationship between tissue modulus (stiffness) times the tissue thickness and resonant frequency determined from OCT and vibrational measurements. Note the cellular components have resonant frequencies less than about 70 Hz and the collagenous components have resoannt frequencies above about 100 Hz.

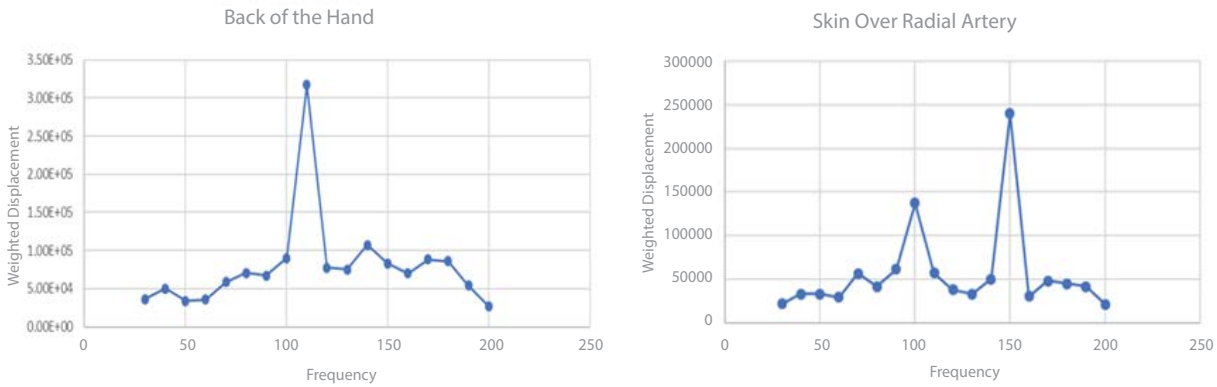

Figure 2: Weighted displacement versus frequency for skin from the back of the hand (left) and from the skin over the radial artery (right) for a subject 69 years old. Note the increased number of peaks from the skin over the radial artery compared to the hand.

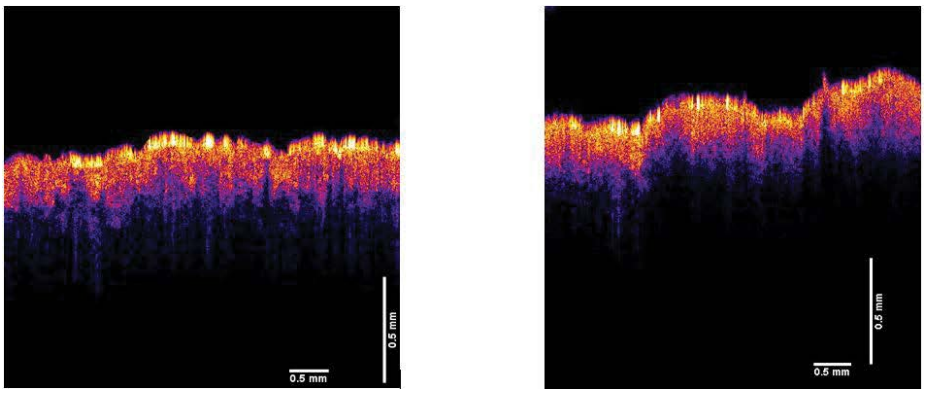

Figure 3: Enhanced OCT image of skin from the wrist for a person aged 25 (left) and from the cheek of a 69 year old person (right). Note the increased undulations in the skin from the older individual.

a plot of weighted displacement versus frequency (Figure 2) and then dividing by the tissue thickness obtained from the OCT image. The weighted displacement was normalized by dividing by the weighted displacement measured in the absence of the sample. The modulus was obtained from the measured resonant frequency and sample thickness and using Figure 1.

The original grayscale OCT images of skin were pseudo color-coded based on the pixel intensities to provide better images of the tissue components as describe previously [16-18]. The enhanced OCT images used darker colored (blue and purple) regions to reflect lower pixel intensities while the lighter (yellowish) regions reflected higher pixel intensity regions.

Skin from ten subjects was studied *in vivo* after informed consent was obtained. The subjects ranged in age from 25 to 75 years of age with a mean age of 57 years old. Tissues examined include skin from the cheek, back of the hand, forehead, palm and skin above the radial artery in the wrist. Some of the subjects were studied before and after they climbed up and down a flight of about 20 stairs until they were winded.

Wrist skin on one subject (69 years old) was subject to application of 20% salicylic acid solution (Walgreens) to remove some of the epidermis.

Results

OCT Images of Skin

Skin was examined using OCT in different areas of the body. Images were color coded based on pixel intensity. As previously reported the OCT images of skin were composed of epidermal and papillary dermal layers which could be identified based on the color and location of the different layers (Figure 3) [14-18]. The color-coded OCT image of skin was found to be dependent on location and age of the subject. In general, skin from younger subjects (24 and 25 years old) had fewer undulations than that of older subjects (60-75 years old); however, this varied from location to location. Images of skin from different locations such as the wrist over the radial artery, cheek, forehead, and palm had thicknesses that varied from about 0.337 mm to 0.594 mm; however, this did not seem to change the cellular or collagen modulus which appears independent of the age of the subject (Table 1).

Removal of the stratum corneum using a 20% salicylic acid solution resulted in a loss of most of the undulations and a decrease in the skin thickness. The thickness of the epidermis and papillary dermis decreased after salicylic acid exposure from 0.588 mm to about 0.336 mm. Scans of forehead and wrist skin illustrated that the cellular content of wrist skin was higher than that of skin from the forehead based on the pixel intensity (Figure 4).

Resonant Frequency, Modulus E, Ratio of Resonant Frequency of Cell/ Collagen					
Tissue	Resonant Frequency (Hz) {SD}	E#1 (MPa) {SD}	E#2 (MPa) {SD}	E#3 (MPa) {SD}	Ratio (Cell/ Collagen)
Wrist	67.5 {13.56}, 110 {7.38}, 155 {11.98}	1.11 {0.25}	2.15 {0.29}	3.66 {0.65}	0.1899
Forehead	75 {7.07}, 134.3 {22.3}	1.45 {0.03}	None	3.25 {1.12}	0.061
Cheek	80, 140	1.30	None	3.22	0.008
Palm	60, 150, 170	0.934	3.31	4.10	0.04
Salicylic acid on Wrist	72.5{5}, 108{4.47}, 158{4.47}	1.201 {0.18}	2.19 {0.23}	4.13 {0.64)	0.24
Fat	40	0.03	None	None	N/A
Melanocytic Nevus	40, 140-180	0.398	None	3.10	12.5
BCC	60, 160	0.618	None	2.66	2.5
AK	70, 140-180	0.890	None	3.05	0.6
SCC	50, 150- 170	0.686	None	2.57	1.1

Normal skin tests were conducted on wrist skin of 10 subjects with an average age of 57. Lesion data was collected from patients 60-70 years old.

Abbreviations used: SD: Standard Deviation, Modulus in MPa: Megapascals, E: Modulus or Stiffness, Hz: hertz, Ratio: Cell resonant frequency peak height/collagen resonant frequency peak height

Note: Ratio of cellular to collagen resonant peak heights is increased in skin lesions

Table 1: Resonant Frequency, Modulus and Ratio of Cellular to Collagen Resonant Frequency Peak Height for Different Locations of Human Skin and Skin Lesions (AK: Actinic Keratosis, BCC: Basal Cell Carcinoma, SCC: Squamous Cell Carcinoma, Melanocytic: Melanocytic Nevus) from this study and references [16-18].

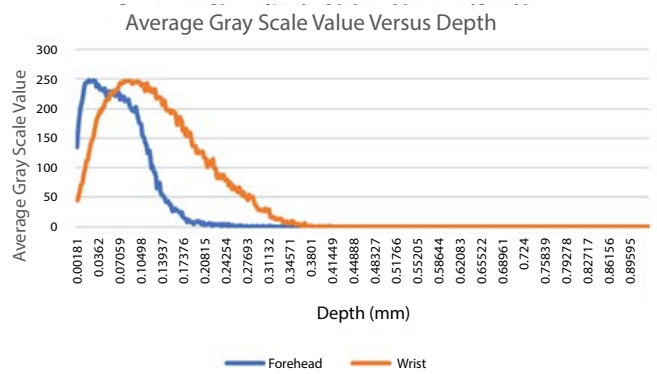

Figure 4: Pixel intensity versus depth for wrist and forehead skin for an individual 59 years old. Note the increased area under the plot for the wrist compared to the forehead. The increased pixel intensity for the wrist indicates an increased cellular and collagen content of this skin compared to the forehead.

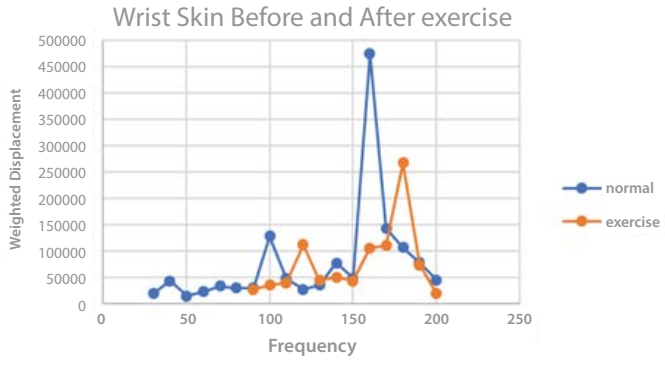

Figure 5: Weighted displacement versus frequency for wrist skin before and after exercise for a 69 year old subject. Note after exercise (walking up and down a flight of stairs several times) the resonant frequencies of all the peaks (cellular, arterial and collagen) observed using VOCT increase suggesting that the pulsatile blood flow in the artery stretches the skin also increasing the modulus. After resting for 1 hour, the peak frequencies observed for wrist skin returned to the preexercise levels. This suggests that the cellular and collagen content of skin may be upregulated by mechanotransduction induced by increased blood flow through the radial artery.

Vibrational study results suggested that the number of resonant frequency peaks found in skin varied from location to location. Cheek skin was characterized by a small resonant frequency peak at about 80 Hz and a collagen peak at 140 Hz while in comparison skin from the wrist over the radial artery had three resonant frequencies: one at about 70 Hz, one at about 110 Hz and one at about 155 Hz (Figure 2 and Table 1). The resonant frequencies and moduli are listed in Table 1 for skin from different regions of the body. When individuals were asked to go up and down the stairs until they were winded, the resonant frequencies of the peaks observed in skin over the radial artery all increased (Figure 5). The resonant frequencies of wrist skin for all individuals returned to the pre-exercise levels after a hour of rest. After salicylic acid treatment, the skin undulations appeared to decrease (Figure 6).

A ratio of the cellular peak height (frequency of 40 to 70 Hz) divided by the collagen peak height for normal skin was less than about 0.06 except for skin in close proximity to the radial artery where it was found to increase to about 0.2 (Table 1). This is in comparison to skin lesions which have ratios that range from 0.6 to 12.5 as reported previously [16,18].

Discussion

The results of this study suggest that skin studied on different parts of the face and wrist from different age groups have different physical characteristics. Wrist skin from young individuals has fewer undulations but in general has similar moduli when compared to collagen in skin from other individuals and other locations (See the modulus E#3 in Table 1). The undulations appear to involve the stratum corneum since when it is removed with salicylic acid the undulations become flattened (Figure 6). However, this didn't appear to affect the tissue modulus. Skin over the

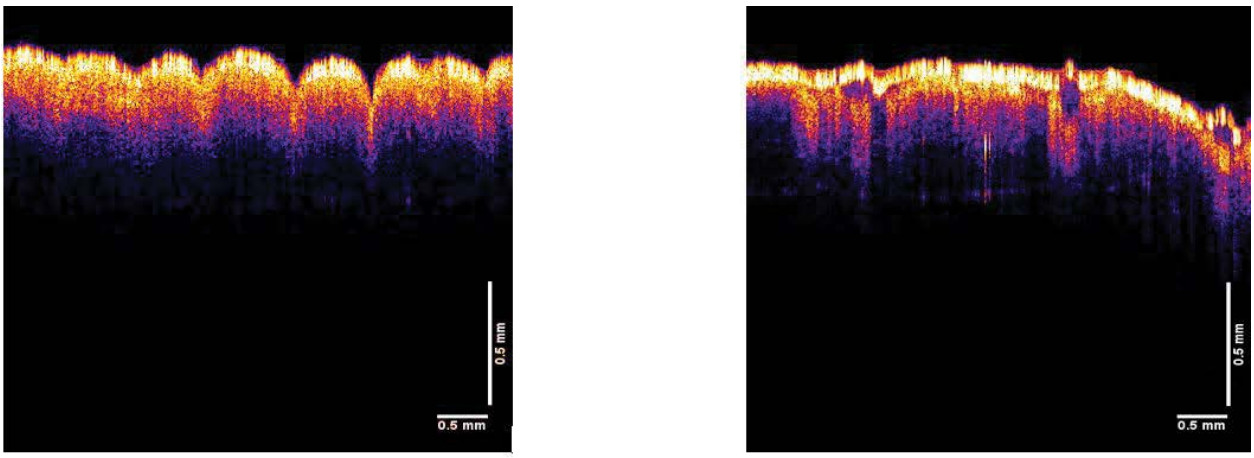

Figure 6: Enhanced OCT image of wrist skin from a 69-year-old subject before (left) and after (right) salicylic acid treatment. A 20% salicylic acid solution was applied to the skin for 30 minutes and then washed off using water. Note the decreased number of undulations in the skin after salicylic acid treatment.

radial artery has three peaks (Figure 2). The peaks include a cellular peak at about 70 Hz, a peak about 110 Hz and one at about 155 Hz. The peak with a resonant frequency of about 110 Hz has modulus of about 2 MPa and appears to reflect the stiffness of the arterial wall. The arterial peak, the cellular and the collagen peaks move to higher frequencies and moduli after exercise (Figure 5). This result suggests that expansion and contraction of the vessel wall induces an increase in the tissue modulus and may be a result of mechanotransduction initiated by the pulsatile blood flow through the radial artery. Increased blood flow may also explain the increased cellular content and peak height of wrist skin compared to facial skin. The ratios of cellular to collagen peak heights appear higher for wrist skin than for other areas of normal skin studied (Table 1). This is an important factor for evaluating skin lesions, since the value found for the ratio of cellular to collagen resonant frequency peak heights for skin lesions appears to be above 0.6 as indicated in Table 1.

The change in the ratio of cellular to collagen resonant frequency peak heights appears to be related to the onset of changes previously observed in skin lesions [16-18]. While the cellular peak height increases relative to the collagen, the collagen peak broadens and decreases in height [16,18].

This suggests that in skin lesions the balance between integrin mediated mechanotransduction involving collagen fibers of the ECM and cadherin-cadherin mechanotransduction between cells is somehow altered. The broadening of the collagen peak suggests that matrix remodeling is occurring during lesion formation. The broadness may indicate that the remodeled ECM is oriented differently than normal collagen in the skin; the collagen network in normal skin is observed be biaxially oriented within the plane of the skin [19] while remodeled scar collagen is oriented parallel to the surface of skin.

Several observations suggest that cell-cell and cell-collagen interactions are modulated by cadherins and integrins. These interactions are reported to control spatial signaling inside the cell and ECM remodeling outside the cell [20]. Integrins have been implicated in a number of physical events that occur during normal homeostasis such as responses to stretch, elevated hydrostatic pressure, fluid shear stress, and osmotic forces [21]. Cadherin- and integrin-dependent adhesive specializations have emerged as crucial components of the cellular tension-sensing mechanisms. Their roles include acting as receptors that both transmit mechanical forces and regulate a myriad of intracellular signaling pathways [22].

Both integrins and cadherins are tri-functional; they bind to other cells or to the ECM and provide a means of connection to the cell cytoskeleton and thereby are involved in intracellular signaling [23]. One recent report suggests that alteration of different cadherins and integrins could affect several aspects of cancer progression [24] suggesting that changes in the cell-to-cell and cell to collagen attachments may drive changes in the mechanical properties observed in cancerous lesions.

In addition to integrins and cadherins, linkers of the nucleoskeleton and cytoskeleton (LINC) provide pathways spanning the nuclear envelope (NE) resulting in a direct physical linkage between major cytoskeletal and nucleoskeletal elements. The ability of LINC complexes to sense and transmit cytoskeletal forces across the NE is critical for force transmission into and out of the cell and cell nucleus [25].

This link between the cell nucleus through LINC complexes may help to explain why a recent report indicates that temporary loading prevents cancer progression and immune organ atrophy induced by hind-limb unloading in mice [26]. However, whether changes in LINC complexes, DNA, cadherins, integrins, collagen of the ECM or mechanical loading are the mediators or cofactors in cancer formation and metastasis, it is clear that these changes are associated with increases in the amount, alignment and densification of collagen in the ECM [27].

Due to exposure to UV light, the collagen matrix and the genetic material of the cell or both, cause an alteration in the

cell-cell and cell-collagen interactions; however, it is clear that cleavage of collagen fibers in skin associated with aging may influence the mechanical link *via* integrins to the cell membrane. This alteration may be transduced to the cell cytoskeleton and nucleus which could alter the transmission of mechanical forces between cells *via* the adherence junctions and to the ECM *via* integrin binding sites. How ECM extracellular tension and collagen fragmentation are involved in lesion formation is unclear; however, using VOCT it is possible to study changes in the cell-collagen relationships *in vivo* observed in different skin lesions and diseases.

Conclusion

The biomechanical relationship between cells and collagen found in skin is complex. In areas of skin not affected by pulsatile blood flow, the cellular resonant frequency peak observed by VOCT is hard to detect. In areas of skin near arteries, there appears to be an increased cellular resonant frequency peak height that may be due to mechanotransduction as a result of local pulsatile blood flow. In areas not affected by arterial blood flow, the ratio of the cellular resonant frequency peak height to the collagen resonant frequency peak height increases from about 0.06 to above 0.6 in pre-cancerous and cancerous lesions. This increased ratio of the cellular to collagen resonant frequency peak height may reflect a change in the balance of force transduction mediated by integrins and cadherins and may lead to both collagen catabolism and cellular proliferation due to environmental and mechanical changes that affect the phosphokinase pathways. The balance between mechanically induced cadherin to cadherin interactions and integrin to collagen interactions may drive alterations in the phosphokinase pathways that lead to cellular proliferation and collagen remodeling observed in cancerous skin lesions.

Reference

1. Silver FH, Siperko LM (2003) Mechanosensing and Mechanochemical Transduction. Critical Reviews in Biomedical Engineering 31: 255-331.
2. Saxena V, Huang C-W, Huang S, Eichbaum Q, Ingber D, et al. (2004) Vacuum assisted closure: microdeformations of wounds and cell proliferation. Plast Reconst Surg 114: 1086-1096.
3. Rosineczuk J, Taradaj J, Dymarek R, Sopel M (2016) Mechanoregulation of wound healing and skin homeostasis. BioMed Res Int.
4. Ng TL, Kersh ME, Kilbreath S, Tate HK (2017) Establishing the basis for mechanobiology based physical therapy protocols to potentiate cellular healing and tissue regeneration. Front Physiol 8: 3030.
5. Silver FH (2006) Mechanosensing and Mechanochemical Transduction in Extracellular Matrix. Springer, NY.
6. Najrana T, Sanchez-Esteban J (2016) Mechanotransduction as an adaptation to gravity. Front Pediatr 4: 140.
7. Silver FH (2017) A matter of gravity-mechanotransduction: how mechanical forces influence biological materials. Material Sci & Eng Int J 1: 00012.
8. Silver FH, Silver LL (2017) Gravity, Mechanotransduction and Healing: How Mechanical Forces Promote Tissue Repair. SM J Biomed Eng. 3(3): 1023.
9. Shah R, DeVore D, Pierce MG (2016) Morphomechanics of dermis-A method for non-destructive testing of collagenous tissues. Skin Res Tech 23: 399-406.
10. Shah R, Pierce MC, and Silver FH (2017) A method for non-destructive mechanical testing of tissues and implants. J Biomed Mat Res 105: 5-22.
11. Silver FH, Silver LL (2017) Non-invasive viscoelastic behavior of human skin and decellularized dermis using vibrational OCT. Derm Clinics & Research 3: 174-179.
12. Shah RG, DeVore D, Silver FH (2018) Biomechanical analysis of decellularized dermis and skin: Initial *in vivo* observations using optical cohesion tomography and vibrational analysis. J Biomed Mat Res 106: 1421-1427.
13. Silver FH, DeVore D, Shah R (2017) Biochemical, biophysical and mechanical characterization of decellularized dermal implants. Material Sciences and Applications 8: 873-888.
14. Silver FH, and Silver LL (2018) Use of Vibrational Optical Coherence Tomography in Dermatology. Archives of Dermatology and Skin Care 1: 03-08.
15. Silver FH, Shah RG, Benedetto D, Dulur A, Kirn T (2019) Virtual biopsy and physical characterization of tissues, biofilms, implants and viscoelastic liquids using vibrational optical coherence tomography. World J Mechanics 9: 11-16
16. Silver FH, Shah RG, Richard M, Benedetto D (2019) Comparative "Virtual Biopsies" of Normal Skin and Skin Lesions Using Vibrational Optical Coherence Tomography. Skin Res Tech 25: 743-749.
17. Silver, FH, Shah, RG, Richard M, Benedetto, D (2019) Comparison of the Virtual Biopsies of a Nodular Basal Cell Carcinoma and an Actinic Keratosis: Morphological, Cellular and Collagen Analyses. Adv Tissue Eng and Regen Med 5: 61-66.
18. Silver, FH, Shah, RG, Richard M, Benedetto, D (2019) Use of Vibrational Optical coherence Tomography to Image and characterize a Squamous Cell Carcinoma. J Derm Res Ther 5: 067.
19. Dunn MG, Silver FH (1983) Viscoelastic behavior of human connective tissues: Relative contribution of viscous and elastic components. Conn Tis Res 12: 59-70.
20. Mui KL, Chen CS, Assoian RK (2016) The mechanical regulation of integrin-cadherin crosstalk organizes cells, signaling and forces. J Cell Sci 129: 1093-1100.
21. Vogel V, Sheetz M (2006) Local force and geometry sensing regulate cell functions. Nat Rev Mol Cell Biol 7: 265-275.
22. Leckband DE, le Duc Q, Wang N, de Rooij J (2011) Mechanotransduction at cadherin-mediated adhesions. Current Opinion in Cell Biology 23: 523-530.
23. Schwartz MA, DeSimone W (2008) Cell adhesion receptors in mechanotransduction. Current Opinion in Cell Biology 20: 551-556.
24. Roggiani F, Mezzanzanica D, Rea K, Tomassetti A (2016) Guidance of Signaling Activations by Cadherins and Integrins in Epithelial Ovarian Cancer Cells. Int J Mol Sci 17: 1387.
25. Jared Z, Fadavi D, Vu UT, Asgari E, Luxton G, et al. (2018) Molecular Insights into the Mechanisms of SUN1 Oligomerization in the Nuclear Envelope. Biophys J 114: 1190-1203.
26. Takahashi A, Wakihata S, Ma L, Adachi A, Hirose H, et al. (2018) Temporary Loading Prevents Cancer Progression and Immune Organ Atrophy Induced by Hind-Limb Unloading in Mice. Int J Mol Sci 19: 3959.
27. Provenzano PP, Eliceiri KW, Jay M Campbell JM, Inman DR, White JG, et al. (2006) Collagen reorganization at the tumor-stromal interface facilitates local invasion. BMC Medicine 4:38.